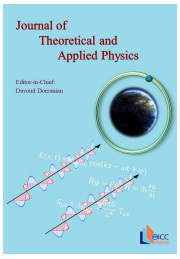

Volume 17, Issue 4, 172342 (1-5)

Journal of Theoretical and Applied Physics (JTAP)

https://dx.doi.org/10.57647/j.jtap.2023.1704.42

Phase transformation; structural and optical properties of Two-Dimensional MoO_3

Mohammad Reza Khanlary *, Azita Keshavarz , Reza Shakoury , Milad Parhizkary

Physics Department of Imam Khomeini International University, Qazvin, Iran.

***Corresponding author**: Khanlary@yahoo.com

Received 25 December 2022; Accepted 03 June 2023; Published online 06 June 2023

Abstract:
Thin-layered materials from transition-metal dichalcogenides family and their preforms such as molybdenum three oxides (MoO_3) exhibit great potential as active material in optoelectronics. Stable materials of few atoms thick have shown emerging capabilities in this area. In this article, we report the synthesis of MoO_3 nanostructures by spray pyrolysis method. We will, perhaps for the first time, show that by varying the hot plate temperature from 350 to 440° C, a phase transformation reveal from h-MoO_3 to α-MoO_3. By annealing the prepared α-MoO_3 sample a preferential orientation of (002) crystal plane is induced. A large bandgap of 2.8 eV for the prepared MoO_3 film was obtained from the transmission spectra. The Raman vibrational modes were investigated for excitation wavelength at 532 nm using MoO_3 films and for a heterostructured MoO_3/MoS_2 film. Better crystallinity and decrease in defects intensity, as an advantage of MoO_3 hybridization can be achieved by proper bfaricating the heterostructure sample.

Keywords: Bandgap; Thin film; Raman spectra; Heterostructure

1. Introduction

The top single, few or even all layers of multiphase materials might have the enough potential to be transformed into another phase by choosing appropriate physical or chemical reactions [1, 2]. Molybdenum trioxide (MoO_3) as semiconductor material with a wide bandgap of ~ 3.2 eV [3] is one of the most interesting transition metal oxides with different forms of crystal structures [4, 5]. Thermodynamically stable orthorhombic phase known as α–MoO_3 is most attractive because of its diverse properties as in super capacitors [6]. Hexagonal h-MoO_3 and monoclinic β– MoO_3 are the metastable phases of n-type MoO_3 semiconductors. MoO_3 nanostructures have a wide application cases such as in lithium-ion batteries [7], catalysts [8], sensors [9], often in the form of a thin film.
It is known that, point defects; such as oxygen vacancies in metastable semiconductors can trap free charge carriers and local excitons. Then, the interaction between these defects and charge carriers is expected to influence physical properties of hosting materials. However, physics and behavior of point defects in 2D semiconductors is much more interesting, as they become stronger at reduced dimensionalities. A 2D MoO_3 film is expected to have a variety of electronic and optical properties different from its bulk structure, originating from phase composition and oxygen stoichiometry, both of which are tunable to obtain desired properties [10]. In the case of α–MoO_3, octahedral are distorted and form bilayers, which build up layered structure. Actually, MoO_6 layers are separated by a Vander Waals gap of dispersed interactions, and oxygen sites on these symmetrically in equivalent sites, singly, doubly and triply coordinated to Mo ions. Generally, different geometries of MoO_3 have been shown to enhance photoluminescence and sensing properties. Exciton bound to defects, if recombine radiatively, lead to light emission at energies lower than the interband optical energies [11]. Meanwhile, binding energy and recombination dynamics of Wannier and Frenkel excitons are expected to be very different for 2D MoO_3.
Molybdenum trioxide can be deposited in a variety of methods; some of these methods are thermal evaporation [12], chemical vapor deposition [13], DC sputtering [14], RF sputtering [15], and atomic layer deposition [16]. The films prepared by each of these methods may not be the same in physical and structural properties due to the different

heating regimes and etc. Among the several approaches available for preparing MoO_3 film, some techniques such as spray pyrolysis are involved to hot substrates.
Owning to the interface issues as well as the multilayer compositions, density of structural defects may increase in the heterogeneous layers [17, 18]. The occurrence of this phenomenon can be justified. In this work, we have studied some structural defects as well as phase transformation of MoO_3 thin films prepared on glass substrate, and compare it to its coating on a MoS_2 substrate, synthesized by the same manner.

2. Experimental

For the deposition of MoO_3 thin films 618 mg of ammonium heptamolybate tetra hydrate [AHM;$(NH_4)_6Mo_7O_{24}.4H_2O$] in 50 ml of deionized distilled water and was stirred about an hour at room temperature. The solution was sprayed onto a clean glass substrate. The substrate temperature was maintained at 350° C. Pyrolytic decomposition of the sprayed solution on the surface of the substrate results in the formation of MoO_3 thin film. The films later on used for the characterization. In a second deposition process the above prepared solution was to another solution containing 0.19 gr of the thiourea [$Sc(NH_2)_2$] powder in 25 mL of deionized water, and stirred for 60 min until reaching a clear colorless solution. Eventually, the solution was sprayed on preheated, the previously MoO_3 thin film as a substrate, at 440° C. In both the spray processes, the interval between nozzle and substrates was ~ 33 cm, and the aqueous solution flow rate was 1 mL/min. A numbers of the samples were annealed in atmospheric oven at 440° C for 60 minutes. Structural properties of the prepared samples was carried out using X-ray diffraction with Cu (Cu Kα) line ($\lambda = 1.54$ $\mathring{A}$). Raman spectra were collected using a Nicolet Almega Dispersive Raman Spectrometer (Thermo Fisher Scientific Inc.) equipped with a maximum power of 100 mW, 532 nm laser. All spectra were collected at 10 mW of power, 32 accumulations.
Optical absorption measurements in the range of $300 - 800$ nm were carried out using a UV-Vis spectrometer (Rayleigh, model UV 2601).

3. Result and discussion

3.1 X-ray diffraction analysis

Fig. 1 shows the XRD spectrum of the MoO_3 film prepared on the heated glass substrate, by the hot plate of the spray unit, at 350° C. The sample product crystalize in the hexagonal phase of MoO_3, and the diffraction peaks are indexed with reference to a standard (JCPDS-21-0569) data file. However, we note that fabricating in this substrate temperature has resulted a highly amorphous film. The highest intense peak observed at $2\theta 27$ is broadened in comparison to the bulk compound. The observed broadening is a combination of the instrument error, the reduced crystallite size and the existence of micro strain in the synthesized sample product. As the h-MoO_3 is thermodynamically metastable, the synthesis of its pure phase is usually more difficult, resulting in that the successful efforts to obtain h-MoO_3 are very limited and thus limit its application. Here it seems that we were successfully able to synthesize, if not pure, but majorly h-MoO_3 phase accompanied with orthorhombic α-MoO_3 thin film. Actually, the prepared sample may be a composition of the hexagonal and orthorhombic MoO_3 (ICCD 01-074-7909). H-MoO_3 has been reported to have reduced crystallite size and grown as one-dimensional.
A phase transformation from h-MoO_3 to α-MoO_3 is reported to occur at 400° C which is in TGA/DTA studies [19]. Therefore, we examined crystallinity of the as-prepared MoO_3 films for the sample made in a higher substrate temperature in the spray unit. The XRD pattern of the sample prepared with a hot plate at 440° C shows (Fig. 2(a)) the polycrystalline nature with the mostly orthorhombic (α-MoO_3) crystal structure. Here, we can see a new relatively high XRD peak value at $2\theta \sim 39$ related to (060) plane of α-MoO_3.
A comparison between the full width at half maximum (FWHM) for (020) of α-MoO_3 and the similar peak for the (040) plane of h-MoO_3 film (Fig. 1), indicate a smaller crystallite size for h-MoO_3 respect to α-MoO3 film with an increase in temperature, the crystallites aggregate and promote rapid growth of the particles. In some research the phase transformation is reported to be occurred in much lower temperature than in the case of the present work but with a longer heating process [20]. No characteristic peaks of the other impurities are observed from this pattern indicating the high purity of prepared sample. However, the wide diffraction peaks suggest that the as-synthesized MoO_3 film is not well crystallized. Amorphous MoO_3 film like some metal oxide films such as TiO_2 film or other nanostructure materials can be transferred to the crystal structure by annealing [16, 21, 22].
We have to note that, temperature and annealing time are important parameters for the transition to the crystalline state and the density of the film changes during annealing. To investigate the effect of the further thermal treatment on the structure properties of the α-MoO_3 sample, XRD pattern of the annealed sample at 440° C was also taken and is shown in Fig. 2(b). Thermal treatment of the α-MoO_3 prepared film, shows the material to be highly crystalline, there were no peak shifts observed relative to the pattern of as-synthesized film. However, two smaller feature which can be related to the h-MoO_3 are now reappeared at $2\theta \sim 32$ and 40.45. The peak at $2\theta \approx 49$, attributed to (020) crystal plane of MoO_3 is now much more intense. Actually, the peak intensities are significantly dependent on the treatment conditions. The origin of such a variation in the XRD peak intensity may be attributed to the change in the preferred crystal orientation, stoichiometry, and defects. An obvious difference in peak intensity at $2\theta \sim 49$ in the annealed sample can also be due to getting the larger crystallite size or obtaining a preferential crystalline orientation with (020) planes, which sometimes occurs in the nanostructures. Here, since the FWHM is not increased by sintering (37 nm before annealing and 36 nm after annealing) it may induced prefer orientation.

It seems that the origin for phase transformation of the metastable phase h-MoO_3 to thermodynamically stable

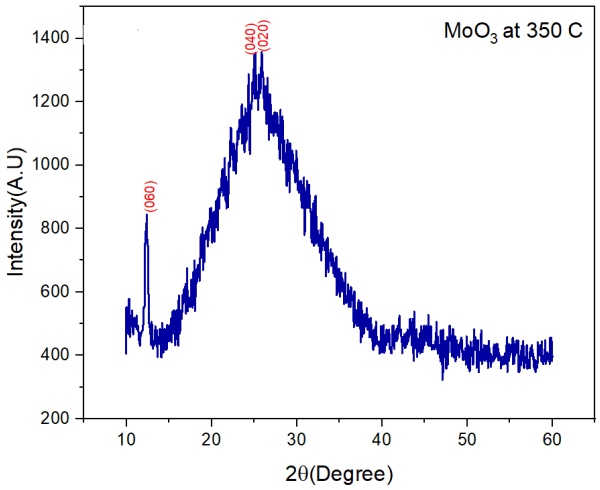

Figure 1. XRD pattern of h-MoO_3 thin films, with substrate temperature at 350° C.

phase α-MoO_3 is due to high temperature heating effect on NH_4^+ Ions during the growth of the α-MoO_3 crystal which occurs in this temperature away from annealing treatment. It has been reported [23] that slow annealing at a temperature of 450° C in an air atmosphere transforms the metastable phase h-MoO_3 to α-MoO_3. This transformation is said to be coherent with the loss of NH_4^+ ions in thermo gravimetric analysis (TGA). After dehydration and removal of ammonia compounds, a sharp exothermic peak at 430° C is attributed to liberation of coordinated water and ammonia molecules from the internal structure of the MoO_3 material, which promotes an irreversible phase transformation from the hexagonal to the orthorhombic structure [24].

3.2 UV-Vis spectroscopy

Fir. 3(a) shows the transmittance spectra in the wavelength region $300-800$ nm for the MoO-3 film deposited at 440° C. Generally, the optical transmission at the transmission edge corresponds to the transition from the valence to the

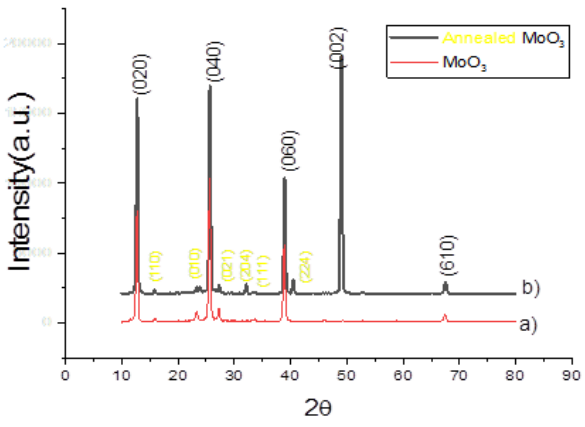

Figure 2. XRD pattern of α-MoO_3 thin films prepared by spray pyrolysis at 440°C substrate temperature (a) as synthesized and (b) after annealing at 440° C.

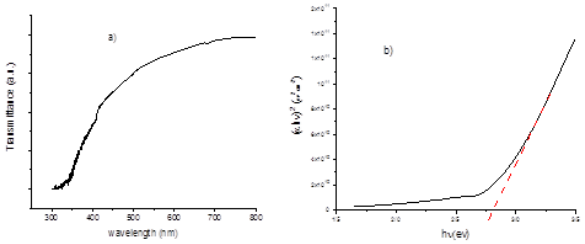

Figure 3. Optical transmission spectra (a) and Tauc's plot of MoO_3 film prepared at 440° C (b).

conduction band, which in our sample has been occurred at energy related to ~ 450 nm. According to this spectra, the MoO_3 bandgap (E_g) is calculated from the Tauc's plot Fig. 5(b). The straight-line portion indicates the direct bandgap in nature. The obtained bandgap is 2.8 eV that is in the range of reported E_g for α-MoO_3 nanostructure [25]. Based on the kinds and their concentration of the structural defects created during the film preparation and their synthesize parameters, variation of E_g values from $2.5-3.2$ eV is reported in the literature [26].

3.3 Raman spectroscopy

MoO_3 offer a highly effective combination with a MoS_2 layer. For MoO_3 is a widely used p-type doping candidate due to the high work function, while MoS_2 is a typical n-type semiconductor featured with low work function. Therefore, it is possible to convert n-type MoS_2 to p-type MoO_3 by partial oxidation reaction. Raman spectroscopy of a composite sample of MoO_3/MoS_2 was applied to monitor the coating treatment of MoO_3 on MoS_2 substrate. Raman spectra of the above mentioned α-MoO_3 film and MoO_3/MoS_2 composite sample with the same manner preparation were collected using 532 nm excitation and are presented in Fig. 4(a) and Fig. 4(b) respectively. The power of the laser was kept sufficiently low to avoid heating effect. Raman active

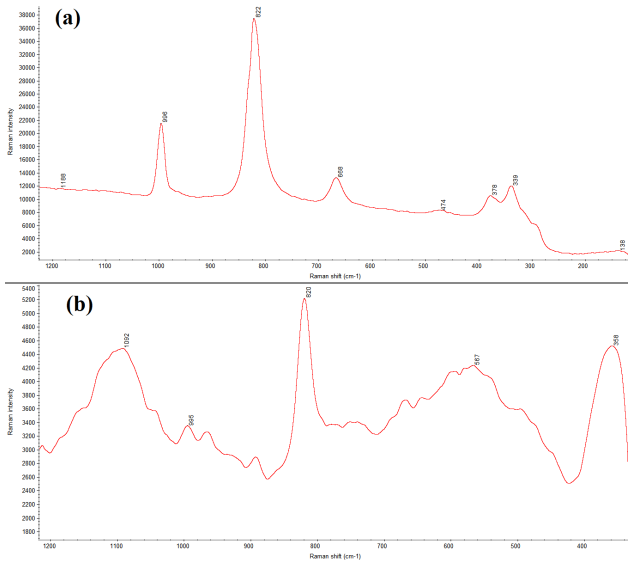

Figure 4. Raman spectra of the (a) α-MoO_3 and (b) MoO_3/MoS_2 prepared samples.

modes identified in Fig. 4(a) confirm the stable orthorhombic phase of MoO_3 [27], with no indication of h-MoO_3 peaks, which are reported to be in 252, 690, 899 and 976 cm^{-1} in the Raman spectrum. We have to note that the energy transfer by laser irradiation process in Raman scatting with this excitation wavelength may cause the omission of low consideration of h-MoO_3 phase in the mixed phases prepared sample. However, there are some features in the Fig. 4(b) with the probability of reappearance the mixture of the both phases in the hydride material. The 285 cm^{-1} (B_{2g}, B_{3g}) band in α-MoO_3 is a doublet comprised of wagging modes of terminal oxygen atoms, the 339 (B_{1g}), 474 (A_g, v_{as} O-M-O stretch and bend are closely resembles for the single crystal Raman spectrum [28]. The 668 cm^{-1} (B_{2g}, B_{3g}) is an asymmetric stretching of the MO-O-MO bridge along the C axis, the 822 cm^{-1} (A_{1g}, B_{1g}) is a symmetric stretch of the terminal oxygen atoms, and the 996 cm^{-1} (A_g, B_{1g}) is the asymmetric stretch of the terminal oxygen atom [29]. Raman peak in the range $830-1130$ cm^{-1} are constructed from up to 3^{rd} order combination of E^1_{2g} (M_2) + A_{1g} (M) subtracted or added to TA(M) or LA(M) phonons. Type of the substrate is known to have noticeable effects on the amount and effectiveness of the defects created during fabrication hybrid nanostructures, causing significant variation on their Raman spectra. Another parameter for controlling structural defects detected by Raman spectra is a thermal treatment, sometimes is required during a thin film sanitization. In a spray pyrolysis process, substrate temperature may play a significant role in the physical properties of the products. One of the consequences of creation the defect in Raman analysis of our hybrid sample is slightly narrowing the main peak of MoO_3 film in 822 cm^{-1} and its redshift in MoO_3/MoS_2 hybrid film. Meanwhile, we believe the new 358 cm^{-1}, 567 cm^{-1} and 1092 cm^{-1} peaks are related to the defects of MoO_3 film created during this new film fabrication. Narrowing, accompanied with a 2 cm^{-1} redshift of the 822 cm^{-1} peak can be related to better crystallinity and decrease in defect density, respectively. These effects are not very clear for other peaks in the figure, indicating no noticeable effect on them by this extra processing on MoO_3 film. MoS_2 is known upon annealing in $\sim 450^\circ$ C by breaking the S-Mo-S bonds create S-vacancies, which facilitate the chemisorption of foreign molecules [30].

4. Conclusion

Sintering effect and phase transformation studies on molybdenum trioxide thin films is done. Fitting the transmission plot with a theoretical curve drives MoO_3 bandgap of 2.8 eV. Raman spectra of MoO_3 and MoO_3/MoS_2 hetrostructured film show mixed phase existence of h-MoO_3 and α-MoO_3 in the prepared samples. The most intense Raman peak known as Ag mode located at 822 cm^{-1} and some other feature familiar Raman active mode of MoO_3 are identified from the analyzed samples. Three additional modes peaked at 358,567 and 1092 cm^{-1} appeared in the MoO_3/MoS_2 film clearly shows the effect of MoS_2 substrate in the prepared MoO_3 film.

Conflict of interest statement:

The authors declare that they have no conflict of interest.

References

[1] L. Li, J. Chena, K. Wu, C. Cao, S. Shi, and J. Cui. "The Stability of Metallic MoS_2 Nanosheets and Their Property Change by Annealing". *Nanomaterials*, **9**:1366, 2019.

[2] M. Khanlary, S. alijarahi, and A. Reyhani. "Growth temperature dependence of VLS-grown ultra-long ZnS nanowires prepared by CVD method". *Theoretical and Applied Physics*, **12**:121, 2018.

[3] A. Khademi, R. Azimirad, A. Zavarian, and A. Moshfegh. "Growth and field emission study of molybdenum oxide nanostars". *The Journal of Physical Chemistry C*, **113**:19298, 2009.

[4] Z. Wang, S. Madhavi, and X. Lou. "Ultralong a-MoO_3 nanobelts: synthesis and effect of binder choice on their lithium storage properties". *The Journal of Physical Chemistry C*, **116**:12508, 2012.

[5] Y. Zhao, J. Liu, Y. Zhou, Z. Zhang, Y. Xu, H. Naramoto, and S. Yamamoto. "Preparation of MoO_3 nanostructures and their optical properties ". *Journal of Physics: Condensed Matter*, **15**:L547, 2003.

[6] J. Li and X. Liu. "Preparation and characterization of α-MoO_3 Nanobelt and its application in supercapacitor ". *Materials Letters*, **112**:39, 2013.

[7] U. Kumar Sen and S. Mitra. "Electrochemical activity of α-MoO_3 nano-belts as lithium-ion battery cathode". *RSC Advances*, **29**:11121, 2012.

[8] E. Gaigneaux, K. Fukui, and Y. Iwasawa. "Morphology of crystalline α-MoO_3 thin films spin-coated on Si (100)". *Thin Solid Films*, **374**:49, 2000.

[9] G. Micocci, A. Serra, A. Tepore, and S. Capone. "Properties of vanadium oxide thin films for ethanol sensor". *Journal of Vacuum Science and Technology A*, **34**:063102, 1997.

[10] H. Hu, C. Deng, J. Xu, K. Zhang, and M. Sun. "Metastable h-MoO_3 and stable α-MoO_3 microstructures: controllable synthesis, growth mechanism and their enhanced photocatalytic activity". *Journal of Experimental Nanoscience*, **10**:1336, 2015.

[11] M. Shahbazi and M. R. Khanlary. "Study of optical, electrochemical, and morphological properties of MoS_2 thin films prepared by thermal evaporation". *Brazilian Journal of Physics*, **51**:1182, 2021.

[12] F. A. Chudnovskii, D. M. Schaefer, A. I. Gavrilyuk, and R. Reifenberger. "A study of the morphology of photochromic and thermochromic MoO_3 morphous films using an atomic force microscope". *Applied Surface Science*, **62**:145, 1992.

[13] A. Abdellaoui, L. Martin, and A. Donnadieu. "Structure and optical properties of MoO_3 thin films prepared by chemical vapor deposition". *physica status solidi A*, **109**:455, 1988.

[14] A. F. Jankowski and L. R. Schrawyer. "Reactive sputtering of molybdenum". *Thin Solid Films*, **193**:61, 1990.

[15] J. Scarminio, A. Lourenço, and A. Gorenstein. "Electrochromism and photochromism in amorphous molybdenum oxide films". *Thin Solid Films*, **302**:66, 1997.

[16] M. F. J. Vos, B. Macco, N. F. W. Thissen, A. A. Bol, and W. M. M. Kessels. "Atomic layer deposition of molybdenum oxide from (NBu)2(NMe2)2Mo and O2 plasma". *Journal of Vacuum Science and Technology A*, **34**:103, 2016.

[17] D. Scirè, P. Proce, A. Gulino, O. Isabella, M. Zeman, and I. Crupi. "Sub-gap defect density characterization of molybdenum oxide: An annealing study for solar cell applications". *Nano Research*, **13**:3416, 2020.

[18] M. Khanlary and S. Tarzi. "Study of structural, optical and morphological properties of ZnO/ZnS hetrostructures deposited by spray pyrolysis method". *Optical and Quantum Electronics*, **53**:1, 2021.

[19] J. Song, X. Ni, L. Geo, and H. Zheng. "Synthesis of Metastable h-MoO_3 by Simple Chemical Precipitation". *Materials Chemistry and Physics*, **102**:245, 2007.

[20] T. Nagyné-Kovács, L. Studnicka, I. Endre Lukács, K. László, P. Pasierb, I. Miklós Szilágyi, and G. Pokol. "Hydrothermal Synthesis and Gas Sensing of Monoclinic MoO_3 Nanosheets". *Nanomaterials*, **10**:891, 2020.

[21] S. H. Woo, S. H. Kim, and C. K. Hwangbo. "Optical and structural properties of TiO_2 and MgF_2 thin films by plasma ion-assisted deposition". *Journal of the Korean Physical Society*, **45**:1, 2004.

[22] M. Nikzad, M. Khanlary, and S. Rafee. "Structural, optical and morphological properties of Cu doped ZnS thin films synthesized by sol–gel method ". *Applied Physics A*, **125**:1, 2019.

[23] K. K. Singh, V. Ramakrishnan, R. Prabhu B, and N. S. John. "Rapid augmentation of vertically aligned MoO_3 nanorods via microwave irradiation". *CrystEngComm*, **19**:6568, 2017.

[24] J. Song, X. Ni, L. Gao, and H. Zheng. "Synthesis of metastable h-MoO_3 by simple chemical precipitation". *Materials Chemistry and Physics*, **102**:245, 2007.

[25] B. Ghasemi, F. Hajakbari, and A. Hojabri. "Structural and optical properties of nanocrystalline MoO_3 thin films grown by thermal oxidation of sputtered molybdenum films". *Inorganic and Nano-Metal Chemistry*, **50**:1, 2020.

[26] D. R. Pereira, C. Díaz-Guerra, M. Peres, S. Magalh, J. G. Correia, J. G. Marques, A. G. Silva, E. Alves, and K. Lorenz. "Shannon entropy for Feinberg–Horodecki equation and thermal properties of improved Wei potential model". *Acta Materialia*, **169**:15, 2019.

[27] M. Mattinen, P. J. King, L. Khriachtchev, M. J. Heikkilä, B. Fleming, S. Rushworth, K. Mizohata, K. Meinander, J. Räisänen, M. Ritala, and M. Leskelä. "Atomic layer deposition of crystalline molybdenum oxide thin films and phase control by post-deposition annealing". *Materials Today Chemistry*, **9**:17, 2018.

[28] M. A. Py and K. Maschke. "Intra- and interlayer contributions to the lattice vibrations in MoO_3". *Physica B*, **105**:370, 1981.

[29] G. Mestl, P. Ruiz, B. Delmon, and H. Knozinger. "Oxygen-exchange properties of MoO_3: an in situ Raman spectroscopy study". *The Journal of Physical Chemistry*, **98**:11269, 1994.

[30] M. Donarelli, F. Bisti, F. Perrozzi, and L. Ottaviano. "Tunable sulfur desorption in exfoliated MoS_2 by means of thermal annealing in ultra-high vacuum". *Chemical Physics Letters*, **588**:198, 2013.